NANO LETTERS

Letter

pubs.acs.org/NanoLett

Growth and Anion Exchange Conversion of $CH_3NH_3PbX_3$ Nanorod Arrays for Light-Emitting Diodes

Andrew Barnabas Wong,[†,‡] Minliang Lai,[†] Samuel Wilson Eaton,[†] Yi Yu,[†,‡] Elbert Lin,[†] Letian Dou,[†,‡] Anthony Fu,[†,‡] and Peidong Yang*[,†,‡,⊥,§]

[†]Department of Chemistry and [§]Department of Materials Science and Engineering, University of California, Berkeley, Berkeley, California 94720, United States

[‡]Materials Sciences Division, Lawrence Berkeley National Laboratory, Berkeley, California 94720, United States

[⊥]Kavli Energy Nanosciences Institute, Berkeley, California 94720, United States

Supporting Information

ABSTRACT: The nanowire and nanorod morphology offers great advantages for application in a range of optoelectronic devices, but these high-quality nanorod arrays are typically based on high temperature growth techniques. Here, we demonstrate the successful room temperature growth of a hybrid perovskite ($CH_3NH_3PbBr_3$) nanorod array, and we also introduce a new low temperature anion exchange technique to convert the $CH_3NH_3PbBr_3$ nanorod array into a $CH_3NH_3PbI_3$ nanorod array while preserving morphology. We demonstrate the application of both these hybrid perovskite nanorod arrays for LEDs. This work highlights the potential utility of postsynthetic interconversion of hybrid perovskites for nanostructured optoelectronic devices such as LEDs, which enables new strategies for the application of hybrid perovskites.

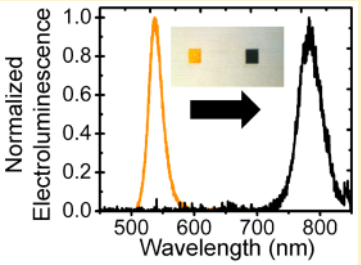

KEYWORDS: *Hybrid perovskite nanorod array, perovskite light-emitting diode, $CH_3NH_3PbBr_3$, $CH_3NH_3PbI_3$, nanorod array light-emitting diode, anion exchange*

Recently, hybrid perovskites such as $CH_3NH_3PbI_3$ and $CH_3NH_3PbBr_3$ have disrupted work on other photovoltaic technologies with efficiencies approaching 20%.[1−4] This class of materials offers remarkable photoluminescence quantum efficiencies (PLQE) up to 70% and minority carrier diffusion lengths up to 175 μm, and these materials can be easily synthesized via low temperature solution processing and with extraordinary band gap tunability.[5,6] In light of this, there have been other proposed uses for these perovskite materials for optoelectronic devices beyond solar cells such as for lasers, photodetectors, and LEDs.[7−12] Previously, thin film LEDs (~15 nm) of $CH_3NH_3PbBr_3$ demonstrated external quantum efficiencies of 0.4% at 530 nm.[10] Although the demonstration of electroluminescence was impressive, it was believed that the efficiency was limited by discontinuities in the thin perovskite film that provide shunt paths.[10] Recently, Li et al. demonstrated electroluminescence with peak external quantum efficiencies reaching 1.2% from hybrid perovskite nanocrystals blended with a thin polyimide dielectric polymer.[12] These results demonstrate the promise of hybrid perovskites for the development of high efficiency solution-processed LEDs.

Nanorod arrays have also been proposed as promising morphologies for LEDs because the vertically oriented nanorod array geometry offers advantages in terms of inherently large active surface area, higher charge carrier injection efficiencies, and improved strain relaxation from thermal expansion caused by heating.[13−16] Surface roughness achieved by etching has been shown to improve the light extraction of conventional light-emitting diodes.[17] The naturally large surface area of nanorod arrays combined with the potential difficulty of planar hybrid perovskite films without inducing damage makes the perovskite nanorod array an ideal platform for hybrid perovskite LEDs. The nanorod array may also act as a waveguide to improve the extraction of light from the active layer.[16,18,19] Overall, nanorod arrays offer a potential means to realize higher external quantum efficiencies for LEDs.

At present, there are limited examples of any device made from hybrid perovskite nanorods or nanowires, although recent work demonstrates their application for solar cells and single nanowire lasers.[20−22] The hybrid perovskites possess a cubic or tetragonal crystal symmetry, which does not favor the crystallization of one-dimensional nanorods. Recently, there have been several examples of hybrid perovskite nanowire synthesis using various approaches.[20−25] In particular, perovskites grown using lead acetate as a precursor have been shown to yield high-quality perovskite crystals, even in aqueous solution.[21,22,26−30] These high-quality hybrid perovskite crystals grown from a lead acetate precursor exhibit a reduced defect density, which makes this precursor an attractive choice for nanorod array synthesis.[21,29,30]

The potential for postsynthetic interconversion and alloying is another fascinating property of the hybrid perovskites. The

Received: May 27, 2015
Revised: July 7, 2015
Published: July 20, 2015

DOI: 10.1021/acs.nanolett.5b02082
Nano Lett. 2015, 15, 5519−5524

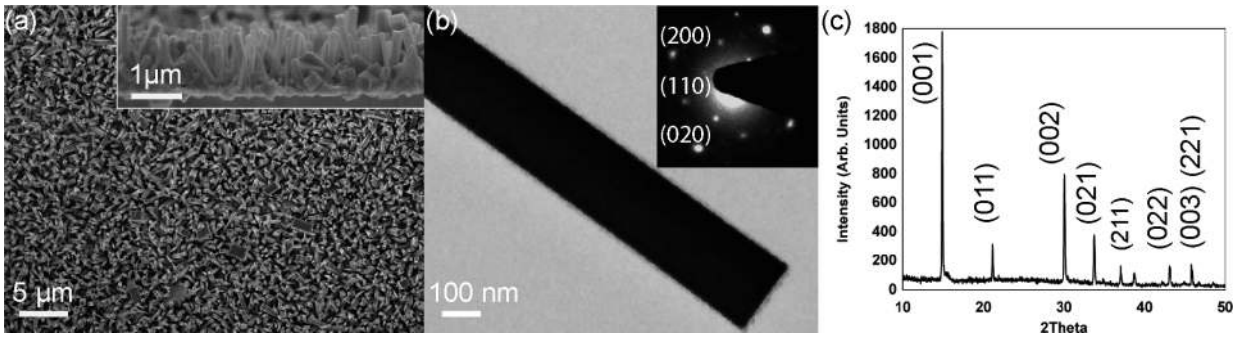

Figure 1. (a) Top view SEM image of $CH_3NH_3PbBr_3$ nanorod array. The inset shows a cross-sectional view of $CH_3NH_3PbBr_3$ array. Inset shows cross-sectional view of $CH_3NH_3PbBr_3$ array. (b) Low magnification TEM image of a $CH_3NH_3PbBr_3$ nanorod with inset showing the SAED of a single nanorod. (c) X-ray diffraction pattern of $CH_3NH_3PbBr_3$ nanorod array.

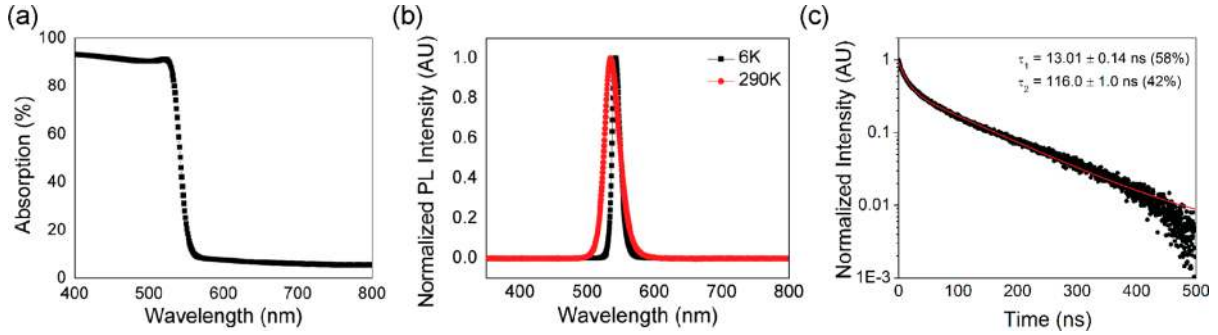

Figure 2. (a) UV−visible absorption spectrum of $CH_3NH_3PbBr_3$ nanorod array grown on Glass/ITO/PEDOT:PSS substrate. (b) PL spectra of $CH_3NH_3PbBr_3$ nanorod array. (c) TRPL of $CH_3NH_3PbBr_3$ nanorod array.

ability to exchange ions has proven to be a highly useful method for the synthesis of new, functional nanostructures.[31−33] The ability to interconvert the halide anion could potentially be another means for controlling the properties toward new functional devices based on hybrid perovskites. However, anion exchanges usually suffer from sluggish reaction kinetics and poor morphology retention, which are attributed to the low mobility and large ionic radius of the anion, so the reaction typically results in hollow particles.[31,34] Recently, Pellet et al. has reported the anion exchange of hybrid perovskite films in the solution phase.[35] This is in agreement with the observation that the photoluminescence of $CH_3NH_3PbI_{3-x}Br_x$ shows photoinduced reversible phase segregation, which likely constitutes a reversible in situ anion exchange.[36] In addition, it has recently been shown that Br_2 and I_2 gas can be used to convert $CH_3NH_3PbI_3$ to $CH_3NH_3PbBr_3$ or $CH_3NH_3PbCl_3$ through redox chemistry.[37] However, to our knowledge, the complete conversion of $CH_3NH_3PbBr_3$ to $CH_3NH_3PbI_3$ has not been previously demonstrated by any method. The ion exchange chemistry of these hybrid perovskites presents a new chemical degree of freedom to explore in the synthesis and application of these materials.

In this work, we demonstrate a solution-phase growth of high quality $CH_3NH_3PbBr_3$ nanorod arrays, which we convert to $CH_3NH_3PbI_3$ nanorod arrays using a simple morphology-preserving anion exchange reaction. Both of these hybrid perovskite nanorod arrays were used to fabricate the first hybrid perovskite nanorod array LEDs as a demonstration of their utility for optoelectronic devices. The structure of the LED device is ITO/PEDOT:PSS/$CH_3NH_3PbX_3$/F8/Ca/Ag, where 9,9-dioctylfluorene (F8) and poly(3,4-ethylenedioxythiophene) polystyrenesulfonate (PEDOT:PSS) are used to facilitate the injection of electrons and holes into the perovskite active layer, respectively.[10,11] In this work, the $CH_3NH_3PbBr_3$ nanorod array exhibits green electroluminescence at 533 nm with a small full width at half maximum (fwhm) of 26 nm. To synthesize $CH_3NH_3PbI_3$ nanorod arrays, the conversion of $CH_3NH_3PbBr_3$ to $CH_3NH_3PbI_3$ by anion exchange was achieved by annealing at 140 to 150 °C in CH_3NH_3I vapor to convert the $CH_3NH_3PbBr_3$ nanorod array into a $CH_3NH_3PbI_3$ nanorod array with retention of the initial morphology. This $CH_3NH_3PbI_3$ also exhibits electroluminescence as an LED at 782 nm, which demonstrates the quality of the $CH_3NH_3PbI_3$ nanorod array produced by anion exchange.

The direct growth of the vertical $CH_3NH_3PbBr_3$ nanorod array is accomplished by coating a saturated methanolic solution of lead acetate onto a PEDOT:PSS coated ITO/glass substrate. This substrate was then placed in a solution of CH_3NH_3Br in 2-propanol to form orange $CH_3NH_3PbBr_3$ nanorod arrays. As shown by scanning electron microscopy (SEM) and transmission electron microscopy (TEM), the individual $CH_3NH_3PbBr_3$ nanorods exhibit a square cross-section with lengths exceeding 1 μm and diameters exceeding 100 nm (Figure 1a,b). Although these nanorods are rapidly damaged by the electron beam in the TEM, the selected area electron diffraction (SAED) pattern shown in the inset of Figure 1b was indexed to the [001] zone axis of cubic $CH_3NH_3PbBr_3$. This SAED pattern reflects that these $CH_3NH_3PbBr_3$ nanorods are single crystalline. The square cross-section of the nanorod reflects the cubic symmetry of the $CH_3NH_3PbBr_3$ unit cell. As shown in the inset cross-sectional SEM image of the $CH_3NH_3PbBr_3$ array, a buffer layer of $CH_3NH_3PbBr_3$ particles with a thickness of over 100 nm also covers the substrate (Figure 1a). The X-ray diffraction (XRD)

DOI: 10.1021/acs.nanolett.5b02082
Nano Lett. 2015, 15, 5519−5524

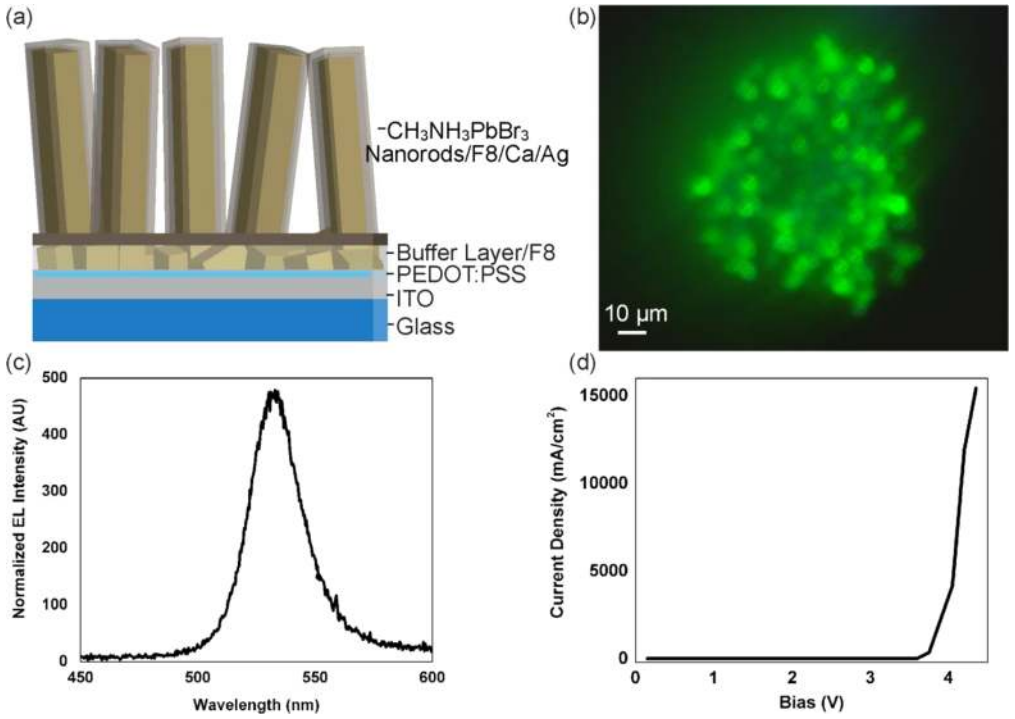

Figure 3. (a) Device structure of a $CH_3NH_3PbBr_3$ nanorod array LED. (b) Image of the electroluminescence from the hybrid perovskite nanorod array LED. (c) Electroluminescence spectrum from the hybrid perovskite nanorod array LED. (d) *IV* characteristic of the hybrid perovskite LED.

pattern of the $CH_3NH_3PbBr_3$ nanorod array can be indexed to cubic phase $CH_3NH_3PbBr_3$ with high phase purity as shown in Figure 1c.

The optical properties of the $CH_3NH_3PbBr_3$ nanorod array highlight their potential for optoelectronic devices. The optical absorption spectrum of the $CH_3NH_3PbBr_3$ nanorod array is shown in Figure 2a. The absorption onset is around 530 nm, which is consistent with the fact that $CH_3NH_3PbBr_3$ is known to have a band gap of 2.3 eV.[38] As shown in Figure 2b, the room temperature photoluminescence of the $CH_3NH_3PbBr_3$ peaks at 534 nm with a relatively narrow fwhm of 26 nm under 325 nm excitation by a HeCd laser. No broad sub-bandgap emission typically associated with defects is observed. The low temperature photoluminescence of the $CH_3NH_3PbBr_3$ at 6 K also exhibits a significant red shift in the photoluminescence to a peak emission at 541 nm with a fwhm of 14 nm, which is a trend opposite of the Varshni relation. In this case, the $CH_3NH_3PbBr_3$ undergoes multiple phase transitions at 236.3 K (to a tetragonal phase), 154.0 K (to another tetragonal phase), and 148.8 K (to an orthorhombic phase), which may account for the observed red shift.[39] The time-resolved photoluminescence shows that the $CH_3NH_3PbBr_3$ nanorod arrays exhibit a biexponential decay with a shorter lifetime of 13.00 ± 0.14 ns and a longer lifetime of 116.0 ± 1.00 ns with 58% and 42% contributions to the biexponential decay function respectively (Figure 2c). It has been proposed that the shorter lifetime corresponds to a surface recombination process while the longer lifetime corresponds to a bulk recombination process.[40,41] Based on previous reports, a bulk crystal of $CH_3NH_3PbBr_3$ has a contribution of approximately 12% of the fast component to the steady state photoluminescence.[40] In comparison, according to this same analysis, the $CH_3NH_3PbBr_3$ nanorod array has a 13% contribution of the fast component to the steady state photoluminescence, which indicates the high quality of the single-crystalline nanorods within the nanorod array.

The fabrication of the nanorod array perovskite LED adapts previous reports for planar devices, which utilized PEDOT:PSS as an ohmic hole injection layer and Ca/F8 as an electron injection layer.[10,12] The device consists of ITO/PEDOT:PSS/$CH_3NH_3PbBr_3$/F8/Ca/Ag as shown in the illustration in Figure 3a. After the growth of the perovskite array on the PEDOT:PSS coated ITO, the $CH_3NH_3PbBr_3$ nanorod array is coated with F8, which allows for electron transport while preventing quenching of emission at the interface with Ca metal.[10] Afterward, 100 nm of Ca and 300 nm of Ag is thermally evaporated to coat the nanorod array and enable electrical contact between nanorods, as shown via SEM in Supporting Information, Figures S1 and S2. The metal is evaporated through a shadow mask to allow for individually addressable metal contacts between different microscale devices on the nanorod array LEDs.

For these devices, the turn-on voltage for room temperature electroluminescence is around 3.5 V of DC bias, which is 0.2 V higher than the thin film case.[10] This difference may be due to the increased contact area of the nanorod array relative to the thin film.[42] The electroluminescence observed from the perovskite devices is strikingly green as shown in the image as well as the spectrum of the electroluminescence (Figures 3b,c). The image of the electroluminescence was collected through the ITO/glass substrate using an inverted optical microscope. The spectrum of the electroluminescence is centered around 533 nm with a fwhm of approximately 26 nm, which indicates good color purity. This fwhm is identical to the fwhm of the photoluminescence emission, which suggests that there is good hole and electron injection into the active layer. It is notable that there is no electroluminescence that could be attributed to F8 in this device, which confirms that the role of F8 is for electron transport to the active $CH_3NH_3PbBr_3$.

DOI: 10.1021/acs.nanolett.5b02082
Nano Lett. 2015, 15, 5519−5524

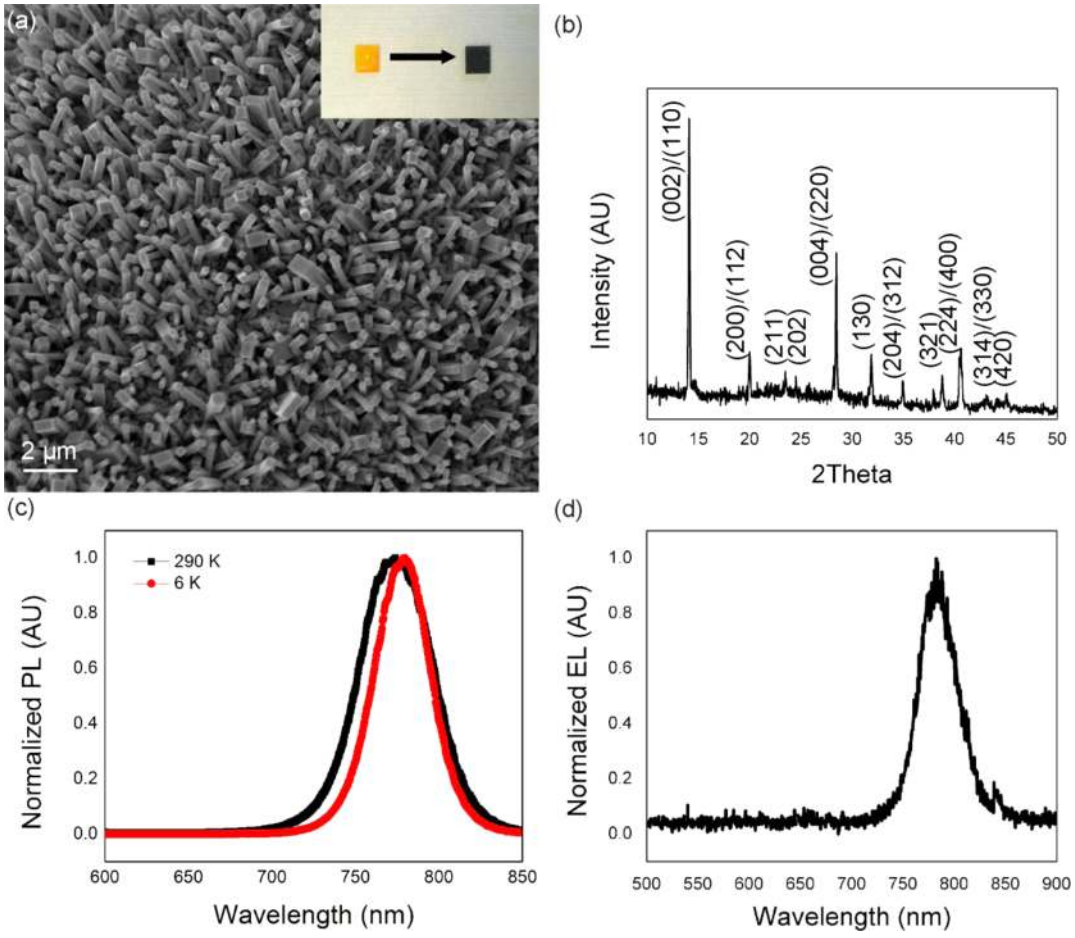

Figure 4. (a) $CH_3NH_3PbI_3$ nanorod array formed by vapor phase anion exchange of $CH_3NH_3PbBr_3$ nanorod array. The inset shows a photograph of a converted chip. (b) XRD pattern of $CH_3NH_3PbI_3$ from anion exchange. (c) Normalized photoluminescence of $CH_3NH_3PbI_3$ nanorod array after conversion. (d) Electroluminescence spectrum of $CH_3NH_3PbI_3$ LED.

Both the electroluminescence image and the spectrum were collected at 10 and 8 V of bias respectively using DC pulses lasting 100 ms and spaced 200 ms apart. As seen in Figure 3d, the DC current density may exceed 10 A/cm^2. This current density was estimated based on the dimensions of the electrode, which closely match with the areas exhibiting electroluminescence such as in Figure 3b. These high current densities can lead to rapid device failure caused by Joule heating. Although this current density is high, it is notable that this value is within an order of magnitude of the current densities reported for planar thin film $CH_3NH_3PbI_{3-x}Cl_x$ LEDs.[10] As shown by Tan et al., the measurement range for the bias can be extended by applying a pulsed DC bias to the LEDs. Under a pulsed DC bias, light emission from the nanorod array LED continues on the time scale of several minutes when tested in ambient air. Untested LEDs remain viable in ambient air for at least 12 h under low humidity (less than 42%). Improvements to the stability of the device while emitting light as well as improvements to the efficiency remain areas of active study.

To synthesize the $CH_3NH_3PbI_3$ nanorod arrays, the anion exchange to form $CH_3NH_3PbI_3$ from $CH_3NH_3PbBr_3$ has been investigated. By annealing the $CH_3NH_3PbBr_3$ nanorod array in CH_3NH_3I vapor at 150 °C, anion exchange to slowly form a $CH_3NH_3PbI_3$ nanorod array is possible. The excess of CH_3NH_3I provides the driving force for the anion exchange reaction. As shown in Figure 4a, the nanorod morphology can be retained after the vapor phase anion exchange reaction. The inset photo illustrates the striking conversion of the nanorod arrays from orange $CH_3NH_3PbBr_3$ to black $CH_3NH_3PbI_3$. After the anion exchange conversion, the $CH_3NH_3PbI_3$ nanorods remain single-crystalline as measured by SAED (Figure S3). The phase purity of the $CH_3NH_3PbI_3$ nanorod array was confirmed by XRD (Figure 4b). The XRD pattern can be fully indexed to the tetragonal phase of $CH_3NH_3PbI_3$. The photoluminescence properties of these films were also investigated, and no photoluminescence from $CH_3NH_3PbBr_3$ remained after the reaction was completed. At room temperature, the $CH_3NH_3PbI_3$ nanorod arrays exhibit photoluminescence at 774 nm with a fwhm of 51 nm, which is shown in Figure 4c. To our knowledge, this result is the most complete conversion of $CH_3NH_3PbBr_3$ to $CH_3NH_3PbI_3$ achieved so far. By controlling the reaction time, alloy compositions of the nanorod arrays can be achieved. The photoluminescence of $CH_3NH_3PbI_xBr_{3-x}$ nanorod arrays formed by partial anion exchange is shown in Figure S4a with a spectrum demonstrating electroluminescence at 551.5 nm as shown in Figure S4b. For low temperature photoluminescence of fully converted $CH_3NH_3PbI_3$, as in the case with the $CH_3NH_3PbBr_3$, a phase transition exists at 162.2 K from tetragonal to orthorhombic, which may influence the low temperature peak position (779 nm, fwhm 39 nm). This small red shift is in agreement with reports on the low temperature photoluminescence of $CH_3NH_3PbI_3$ exhibiting an initial blue shift

DOI: 10.1021/acs.nanolett.5b02082
Nano Lett. 2015, 15, 5519−5524

caused by the phase transition with a further red shifting of the emission with decreasing temperatures.[43−45] The broad low temperature emission of the $CH_3NH_3PbI_3$ has been attributed to homogeneous line broadening caused by phonon-coupling effects as well as by the proposed coexistence of the low temperature and room temperature phases of $CH_3NH_3PbI_3$ below the phase transition.[43,44]

Finally, this $CH_3NH_3PbI_3$ nanorod array formed by anion exchange was applied to demonstrate room temperature electroluminescence in a device stack with an identical configuration to the $CH_3NH_3PbBr_3$ LED. These devices exhibit a much lower short circuit current density (on the order of 1 mA/cm^2) due to the increased resistivity of the LED (Figure S5). The electroluminescence shown in Figure 4d was observed at a bias of 15 V under a pulsed DC measurement. The emission is centered in the infrared at 782 nm with a fwhm of 41 nm, which means that all of the light emission is beyond the 720 nm limit of visible light that can be seen by the human eye. Overall, this result represents a first example of the use of anion exchange to produce new morphological control over the growth of $CH_3NH_3PbI_3$, which can be applied for functional devices.

In summary, we have demonstrated the first solution synthesis of $CH_3NH_3PbBr_3$ perovskite nanorod arrays at room temperature and a new and straightforward anion exchange reaction to form $CH_3NH_3PbI_3$ nanorod arrays. Both of these nanorod arrays exhibit electroluminescence at room temperature. This work identifies the potential for the application of postsynthetic conversion chemistry to modify nanostructured hybrid perovskites for optoelectronic devices such as LEDs. In the future, it may be possible to apply this anion exchange technique to other systems in order to realize other types of optoelectronic devices.

■ ASSOCIATED CONTENT

Supporting Information

Experimental methods, SEM images of LED, electron diffraction of nanorods after anion exchange, photoluminescence and electroluminescence of $CH_3NH_3PbI_xBr_{3-x}$ nanorod arrays, *IV* characteristic of $CH_3NH_3PbI_3$ nanorod array LED, SEM images illustrating growth conditions, and TEM characterization of $CH_3NH_3PbBr_3$ nanorod coated with F8 polymer. The Supporting Information is available free of charge on the ACS Publications website at DOI: 10.1021/acs.nanolett.5b02082.

■ AUTHOR INFORMATION

Corresponding Author

*(P.Y.) Email: p_yang@berkeley.edu.

Author Contributions

P.Y. and A.B.W. originated the idea for the work. A.B.W., M.L., and E.L. prepared nanorod arrays. A.B.W., M.L., and Y.Y. performed the structural characterization. M.L. performed the device fabrication. A.B.W. and S.W.E. characterized the optical properties of the devices and analyzed the data. The manuscript was written through contributions of all authors. All authors have given approval to the final version of the manuscript.

Funding

This work is supported by Director, Office of Science, Office of Basic Energy Sciences, Materials Sciences and Engineering Division, U.S. Department of Energy under Contract No. DE-AC02-05CH11231(PChem). S.W.E. would like to acknowledge the Camille and Henry Dreyfus Foundation for financial support, award number EP-14-151.

Notes

The authors declare no competing financial interest.

■ REFERENCES

(1) Zhou, H.; Chen, Q.; Li, G.; Luo, S.; Song, T.-B.; Duan, H.-S.; Hong, Z.; You, J.; Liu, Y.; Yang, Y. *Science* **2014**, *345*, 542−546.
(2) Lee, M. M.; Teuscher, J.; Miyasaka, T.; Murakami, T. N.; Snaith, H. J. *Science* **2012**, *338*, 643−647.
(3) Burschka, J.; Pellet, N.; Moon, S.-J.; Humphry-Baker, R.; Gao, P.; Nazeeruddin, M. K.; Grätzel, M. *Nature* **2013**, *499*, 316−319.
(4) Jeon, M. J.; Noh, J. H.; Yang, W. S.; Kim, Y. C.; Ryu, S.; Seo, J.; Seok, S. I. *Nature* **2015**, *517*, 476−480.
(5) Deschler, F.; Price, M.; Pathak, S.; Klintberg, L. E.; Jarausch, D.-D.; Higler, R.; Hüttner, S.; Leijtens, T.; Stranks, S. D.; Snaith, H. J.; Atatüre, M.; Phillips, R. T.; Friend, R. H. *J. Phys. Chem. Lett.* **2014**, *5*, 1421−1426.
(6) Dong, Q.; Fang, Y.; Shao, Y.; Mulligan, P.; Qiu, J.; Cao, L.; Huang, J. *Science* **2015**, *347*, 967−970.
(7) Zhang, Q.; Ha, S. T.; Liu, X.; Sum, T. C.; Xiong, Q. *Nano Lett.* **2014**, *14*, 5995−6001.
(8) Sutherland, B. R.; Hoogland, S.; Adachi, M. M.; Wong, C. T. O.; Sargent, E. H. *ACS Nano* **2014**, *8*, 10947−10952.
(9) Dou, L.; Yang, Y. M.; You, J.; Hong, Z.; Chang, W.-H.; Li, G.; Yang, Y. *Nat. Commun.* **2014**, *5*, 5404.
(10) Tan, Z.-K.; Moghaddam, R. S.; Lai, M. L.; Docampo, P.; Higler, R.; Deschler, F.; Price, M.; Sadhanala, A.; Pazos, L. M.; Credgington, D.; Hanusch, F.; Bein, T.; Snaith, H. J.; Friend, R. H. *Nat. Nanotechnol.* **2014**, *9*, 687−692.
(11) Wang, J.; Wang, N.; Jin, Y.; Si, J.; Tan, Z.-K.; Du, H.; Cheng, L.; Dai, X.; Bai, S.; He, H.; Ye, Z.; Lai, M. L.; Friend, R. H.; Huang, W. *Adv. Mater.* **2015**, *27*, 2311−2316.
(12) Li, G.; Tan, Z.-K.; Di, D.; Lai, M. L.; Jiang, L.; Lim, J. H.-W.; Friend, R. H.; Greenham, N. C. *Nano Lett.* **2015**, *15*, 2640−2644.
(13) Li, S.; Waag, A. *J. Appl. Phys.* **2012**, *111*, 071101.
(14) Chen, C.-H.; Chang, S.-J.; Chang, S.-P.; Li, M.-J.; Chen, I.-C.; Hsueh, T.-J.; Hsu, C.-L. *Appl. Phys. Lett.* **2009**, *95*, 223101.
(15) Sheu, J.-K.; Lu, Y. S.; Lee, M.-L.; Lai, W. C.; Tun, C.-J. *Appl. Phys. Lett.* **2007**, *90*, 263511.
(16) Lupan, O.; Pauporté, T.; Viana, B. *Adv. Mater.* **2010**, *22*, 3298−3302.
(17) Fujii, T.; Gao, Y.; Sharma, R.; Hu, E. L.; DenBaars, S. P.; Nakamura, S. *Appl. Phys. Lett.* **2004**, *84*, 855−857.
(18) Zhong, J.; Chen, H.; Saraf, G.; Lu, Y.; Choi, C. K.; Song, J. J.; Mackie, D. M.; Shen, H. *Appl. Phys. Lett.* **2007**, *90*, 203515.
(19) Lai, E.; Kim, W.; Yang, P. *Nano Res.* **2008**, *1*, 123−128.
(20) Im, J.-H.; Luo, J.; Franckevicius, M.; Pellet, N.; Gao, P.; Moehl, T.; Zakeeruddin, S. M.; Nazeeruddin, M. K.; Gratzel, M.; Park, N. G. *Nano Lett.* **2015**, *15*, 2120−2126.
(21) Zhu, H.; Fu, Y.; Meng, F.; Wu, X.; Gong, Z.; Ding, Q.; Gustafsson, M. V.; Trinh, M. T.; Jin, S.; Zhu, X.-Y. *Nat. Mater.* **2015**, *14*, 636−642.
(22) Fu, Y.; Meng, F.; Rowley, M. B.; Thompson, B. J.; Shearer, M. J.; Ma, D.; Hamers, R. J.; Wright, J. C.; Jin, S. *J. Am. Chem. Soc.* **2015**, *137*, 5810−5818.
(23) Horváth, E.; Spina, M.; Szekrényes, Z.; Kamarás, K.; Gaal, R.; Gachet, D.; Forró, L. *Nano Lett.* **2014**, *14*, 6761−6766.
(24) Zhu, F.; Men, L.; Guo, Y.; Zhu, Q.; Bhattacharjee, U.; Goodwin, P. M.; Petrich, J. W.; Smith, E. A.; Vela, J. *ACS Nano* **2015**, *9*, 2948−2959.
(25) Deng, H.; Dong, D.; Qiao, K.; Bu, L.; Li, B.; Yang, D.; Wang, H.-E.; Cheng, Y.; Zhao, Z.; Tang, J.; Song, H. *Nanoscale* **2015**, *7*, 4163−4170.
(26) Poglitsch, A.; Weber, D. *J. Chem. Phys.* **1987**, *87*, 6373−6378.
(27) Aldibaja, F. K.; Badia, L.; Mas-Marzà, E.; Sánchez, R. S.; Barea, E. M.; Mora-Sero, I. *J. Mater. Chem. A* **2015**, *3*, 9194−9200.

DOI: 10.1021/acs.nanolett.5b02082
Nano Lett. 2015, 15, 5519−5524

(28) Pisoni, A.; Jaćimović, J.; Barišić, O. S.; Spina, M.; Gaál, R.; Forró, L.; Horváth, E. J. *J. Phys. Chem. Lett.* **2014**, *5*, 2488−2492.
(29) Zhang, W.; Saliba, M.; Moore, D. T.; Pathak, S. K.; Hörantner, M. T.; Stergiopoulos, T.; Stranks, S. D.; Eperon, G. E.; Alexander-Webber, J. A.; Abate, A.; Sadhanala, A.; Yao, S.; Chen, Y.; Friend, R. H.; Estroff, L. A.; Wiesner, U.; Snaith, H. J. *Nat. Commun.* **2015**, *6*, 6142.
(30) Buin, A.; Pietsch, P.; Xu, J.; Voznyy, O.; Ip, A. H.; Comin, R.; Sargent, E. H. *Nano Lett.* **2014**, *14*, 6281−6286.
(31) Beberwyck, B. J.; Surendranath, Y.; Alivisatos, A. P. *J. Phys. Chem. C* **2013**, *117*, 19759−19770.
(32) Tang, J.; Huo, Z.; Brittman, S.; Gao, H.; Yang, P. *Nat. Nanotechnol.* **2011**, *6*, 568−572.
(33) Zhang, D.; Wong, A. B.; Yu, Y.; Brittman, S.; Sun, J.; Fu, A.; Beberwyck, B.; Alivisatos, A. P.; Yang, P. *J. Am. Chem. Soc.* **2014**, *136*, 17430−17433.
(34) Park, J.; Zheng, H.; Jun, Y.-W.; Alivisatos, A. P. *J. Am. Chem. Soc.* **2009**, *131*, 13943−13945.
(35) Pellet, N.; Teuscher, J.; Maier, J.; Grätzel. *Chem. Mater.* **2015**, *27*, 2181−2188.
(36) Hoke, E. T.; Slotcavage, D. J.; Dohner, E. R.; Bowring, A. R.; Karunadasa, H. I.; McGehee, M. D. *Chem. Sci.* **2015**, *6*, 613−617.
(37) Solis-Ibarra, D.; Smith, I. C.; Karunadasa, H. I. *Chem. Sci.* **2015**, *6*, 4054−4059.
(38) Edri, E.; Kirmayer, S.; Kulbak, M.; Hodes, G.; Cahen, D. *J. Phys. Chem. Lett.* **2014**, *5*, 429−433.
(39) Gesi, K. *Ferroelectrics* **1997**, *203*, 249−268.
(40) Shi, D.; Adinolfi, V.; Comin, R.; Yuan, M.; Alarousu, E.; Buin, A.; Chen, Y.; Hoogland, S.; Rothenberger, A.; Katsiev, K.; Losovyj, Y.; Zhang, X.; Dowben, P. A.; Mohammed, O. F.; Sargent, E. H.; Bakr, O. M. *Science* **2015**, *347*, 519−522.
(41) Zhang, F.; Zhong, H.; Chen, C.; Wu, X.-G.; Hu, X.; Huang, H.; Han, J.; Zou, B.; Dong, Y. *ACS Nano* **2015**, *9*, 4533−4542.
(42) Kim, H.-M.; Cho, Y.-H.; Lee, H.; Kim, S. I.; Ryu, S. R.; Kim, D. Y.; Kang, T. W.; Chung, K. S. *Nano Lett.* **2004**, *4*, 1059−1062.
(43) Wehrenfennig, C.; Liu, M.; Snaith, H. J.; Johnston, M. B.; Herz, L. M. *APL Mater.* **2014**, *2*, 081513.
(44) Yamada, Y.; Nakamura, T.; Endo, M.; Wakamiya, A.; Kanemitsu, Y. *IEEE J. of Photovoltaics* **2015**, *5*, 401−405.
(45) Xing, J.; Liu, X. F.; Zhang, Q.; Ha, S. T.; Yuan, Y. W.; Shen, C.; Sum, T. C.; Xiong, Q. *Nano Lett.* **2015**, *15*, 4571.

DOI: 10.1021/acs.nanolett.5b02082
Nano Lett. 2015, 15, 5519−5524